Indian Journal of Engineering & Materials Sciences
Vol. 27, October 2020, pp. 1009-1017

Effect on wear property during LN_2 sliding

Anurag Sharma, Ramesh Chandra Singh & Ranganath Muttanna Singari*
Department of Mechanical Engineering, Delhi Technological University, Delhi 110 042, India

Received: 10 November 2019; Accepted: 04 May 2020

In the presented research work the experiments have been performed by using design of experiments (DOE) L_{18} [OA] orthogonal array based on Taguchi S/N (signal-to-noise) ratio. The three control factors namely sliding speed, load and sliding distance varied to three levels (1, 2 and 3), respectively. One control factor has the sliding condition varied to two levels (l= Dry and 2= Cryogenic with LN_2). The dry sliding condition has been made without any coolant. Cryogenic sliding condition has been made by using the direct supply of LN_2 at the interface of pin and disc. Wear volume loss has found to be 45-55% lower during cryogenic cooling with LN_2 as compared with dry sliding. (ANOVA) analysis of variance revealed that sliding condition is having the highest effect of contribution at 64.37%. Field emission scanning electron microscope (FSEM) images of the pins have shown (i) adhesion and edge fracture during dry sliding, (ii) clean and smooth surface found during cryogenic cooling. Field scanning electron microscope (FSEM) images of wear tracks showed (iii) delamination, cavities and plough during dry sliding and (iv) the surface generated during cryogenic sliding was clean with low debris.

Keywords: Dry sliding, Cryogenic sliding, Temperature, Wear, Optimization, ANOVA

1 Introduction

Traditional coolants and lubricants may be inadequate in providing low wear volume between tribopairs like ball bearings, gears, levers etc. operating at high speed in extreme pressure and load in spacecraft, aircraft and submarines. Cryogenic cooling could be done by liquid nitrogen, helium, hydrogen and solid carbon dioxide. This may be done by circulating cryogenic fluid either in the closed ducts passing over the enclosed chamber or directly supply at the interface of pin and disc[1-5]. Liquid nitrogen is tasteless, odourless, colourless and non-toxic with the boiling point of LN_2 is -196°C. The atmospheric contact of LN_2 at room temperature (21-25°C) creates white fumes. Liquid nitrogen may not produce harmful effects during contact with the atmosphere. The health-related issues of an operator like breathing problems, nausea, skin infections, inflammation to hands and eyes etc., may be resolved[6-9].The debris generated were free from oil content or another type of harmful substance which may be difficult to remove. The scrape of material could be readily used as a source of direct recycling. This could be cost saving in handling and cleaning of debris from oil and harmful substances from coolants[10-12]. Specially designed cryotribometers made by Federal Institute of Materials Research and Testing Institute for investigating material behaviour and tribological properties at various ranges of speed, load and distance in the presence of LN_2 and LHe from 71 - 4.2 °K[13-16]. This could simulate dry sliding and submerged coolant sliding conditions. The wear rate during liquid nitrogen was low as compared to dry sliding[17]. Cooling was maintained by closed ducts through circulating LN_2 around the closed chamber of pin-on-disc tribometer by Ostrovskaya *et al.*[18] for analysing the tribological changes in properties in the vacuum temperature range of 293-77°K. Graphite and diamond were investigated in the temperature range of 4.2-293°K. In diamond (pin) - CVD coated diamond disc, coefficient of friction was maximum at 4.2°K and decreased with temperature but in graphite (pin) - CVD coated diamond disc, coefficient of friction varied with temperature in mid-temperature range. This may be due to wear particles generated by graphite pin[19]. Lubrication properties of molybdenum were investigated by Dunkle *et al.*[20] in vacuum cryogenic conditions of 4-300°K for the coefficient of friction and wear properties. Subramonian *et al.*[21] designed a special tribometer for investigating tribological

*Corresponding author: (E-mail: ranganath@dce.ac.in)

properties for ball bearings of rotations of 36000 rpm in a cryogenic environment with LN_2/LHe. Polymers like polyimide (PI), poly-tetrafluoroethylene (PTFE) and polyetheretherketone (PEEK) showed better tribological properties in the presence of LN_2 as compared to room temperature [22-29]. Direct supply of LN_2 at the interface of pin (Ti54) and disc (WC) was used to investigate the wear volume of pin and surface morphology of wear track. A comparison of wear properties was made during dry and cryogenic sliding. It has been found that the wear volume of the pin was low. Wear tracks showed adhesion, galling and plough low during cryogenic sliding[30]. A planned set of experiment with controlled levels of input would give optimized values of output characteristics. This could save wastage of energy and material by eliminating unnecessary hit and trial of experiments. Genichi Taguchi discovered Taguchi technique in 1950[31-32]. This was based on S/N (signal-to-noise) ratio. In the presented collection of research work, steel like AISI D3, AISI4340, AISI H13, EN19, EN47, white cast iron, titanium alloys and composite materials were used on the Taguchi technique for calculating output characteristics like coefficient of friction, wear volume, wear rate during dry run[33-39]. ANOVA models were proposed to investigate the effect of contribution in terms of percentage. The influence of factor was according to the merit of control factors[40-41]. The review of research papers showed that generally, researchers have used various coatings either on pin or disc, matrix compositions for making pin material, lubricants at the interface of pin and disc for reducing coefficient of friction and wear volume. Some have used cryogenic coolants in closed ducts around the enclosed chamber of pin-on-disc tribometer. This explored the field of different cryogenic fluids like liquid nitrogen, hydrogen, helium and solid carbon dioxide. In the present investigations, AISI D3 (HRC60) steel was used for making the disc. This material is used in manufacturing blanking & forming dies, forming tools, press tools, punches, bushes and wear resistant moulds. It is categorised as difficult to machine materials. TiN coated carbide was used for making the pin. This material was hard and used for making cutting tools. LN_2 was supplied directly at the interface of pin and disc in the closed chamber. Results were optimized by Taguchi(S/N) ratio and ANOVA was used for finding out significant parameters.

2 Materials and Methods

2.1 Disc material

The material used for making circular disc was AISI D3. The diameter and thickness were 165mm and 8mm respectively. Four holes of diameter 5mm were made on disc at the diameter of 150mm. The surface of the disc was grinded. Surface roughness was measured between 0.12 - 0.25µm. R.M.S. value by Taylor Hobson Surtronic 3 + surface roughness tester. Elements (Ets) found in the percentage of weight (wg %) through chemical analysis are shown in Table 1.

2.2 Pin material

The material used for making pin was Tungsten carbide coated with TiN titanium nitride in the cylindrical shape of the diameter of 10 mm and height of 35mm. The coating was in the thickness of 1µm. The elements found in the pin are shown in Table 2.

2.3 Experimental method

A pin-on-disc tribometer was used for the performance of experiments in a dry environment and cryogenic cooling with LN_2 was directly supplied at the interface of pin and disc. The disc could rotate from 200-2000 rpm. The maximum range of frictional force measured was 200N. Figure 1(a) shows the main parts of pin-on-disc tribometer during dry sliding. Hanger was used for carrying the desired weight. Load cell connected with a lever to pin for measuring the frictional force between pin and disc. Figure 1(b) shows that LN_2 was supplied from a dewar container of 55 kg through an insulated

Table 2 — Chemical analysis of carbide pin.

Elets	C	Co	Cr	Fe	W	Ti
Wt%	7.12	12.98	0.045	0.035	30.22	49.6

Table 1 — Elements found through chemical analysis.

Ets	C	Si	Mn	S	P	Cr	Ni	Mo	Co	Nb	V	W	Fe
Wg%	2.03	0.255	0.432	0.026	0.019	11.05	0.073	0.07	0.013	0.021	0.040	0.086	85.525

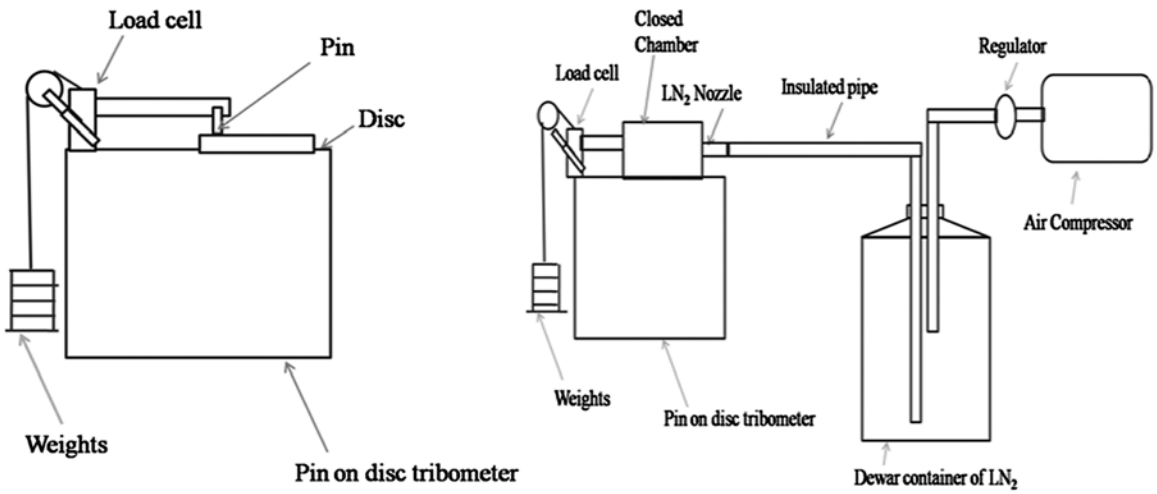

Fig. 1 — Schematic sketch of (a) dry sliding and (b) cryogenic sliding with liquid N_2 .

pipe to the interface of pin and disc in the closed chamber. An air compressor with a regulator was used to supply a controlled amount of air to dewar container.

2.4 Design of Experiment (DoE)

The experiments were performed by using Taguchi orthogonal array [OA], mixed 2-3 level with L_{18} Design of experiments (DoE). The total input control variables were four like sliding speed (SS') (30, 60 and 90m/min.), load (SL') (35, 55 and 75N) and distance (SD') (600, 1200 and 1800m) varied to three levels (1, 2 and 3) respectively. One control factor was varied to two levels (l= Dry and 2= Cryogenic with LN_2). Table 3 shows the details of the control factors. The number of experiments declined to more than 50%. This saved cost related to the raw material of the workpiece, cutting tool, operator and electric power supply.

3 Results and Discussion

3.1 Probability analysis

Figure 2 depicts the probability plot. It is observed that experimental result values obtained are mostly shifted towards the central line and are in the range of normal distribution. P-value is greater than 0.01[39]. This illustrated that further calculations and interpretation of results could be performed.

3.2 Wear Volume

The experiments were performed based on Taguchi L_{18} DoE. Pins were measured on a dedicated measuring scale of least count $\pm 0.0001g$. The

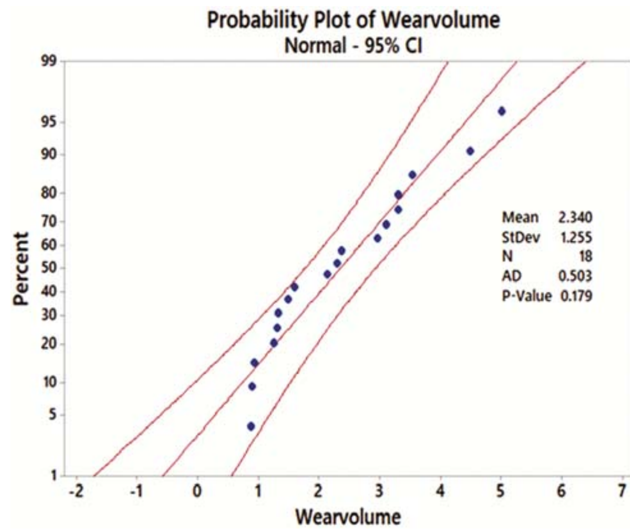

Fig. 2 — Probability plot for wear volume.

Table 3 — Control factors with different level values sliding parameter.

Levels	Sliding Condition	Sliding parameters		
		SS' (m/min.)	SL'(N)	SD'(m)
Level 1	Dry	30	35	600
Level 2	LN_2	60	55	1200
Level 3	-	90	75	1800

difference in weight before and after conducting each experiment was measured and noted. Wear volume loss (Wv') was measured from Eq. 1

$$Wear\ volume\ loss = \frac{Weight\ loss}{Density} \quad \ldots (1)$$

Each experimental run was started with an unused pin for a new wear track on the disc. Wear volume of the pin was found to be low in cryogenic sliding with LN_2 direct supply at the interface of pin and disc as compared to dry sliding as shown in Fig. 3. This may be due to fast heat removing capacity of LN_2[30]. Table 4 shows the respective wear volume loss and the respective S/N ratio value.

3.3 Optimization on the basis of Taguchi (S/N ratio)

Optimization was based on Taguchi S/N ratio. The smaller the better was used in deriving the value of response at the optimum level. This is illustrated in Eq. (2). Table 5 shows S/N values of response (wear volume). Delta is the difference between the highest and lowest value in each control factor. The optimized value is calculated by recognizing the highest value of S/N value of each control factor. Rank is provided showing the influence of factor.

Smaller is the better characteristic

$$\frac{S}{N} = -10log\frac{1}{n}(\sum x^2) \quad \dots (2)$$

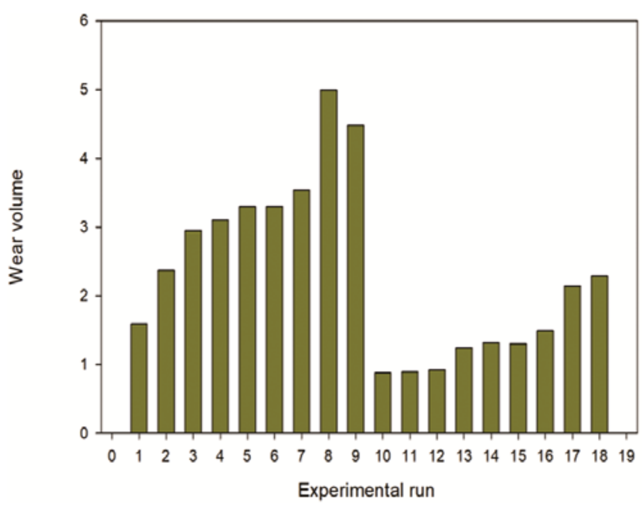

Fig. 3 — Wear volume obtained during experimental run L_{18} DoE.

Diversification of mean S/N ratio Wv' (graphical trend) according to input control factors has been shown in Fig. 4(a) and numerical values in Table 5, respectively. Diversification of mean Wv'(graphical trend) according to input control factors have been shown in Fig. 4(b) and numerical values in Table 6 respectively. On incrementing speed, load and

Table 4 — L_{18} Taguchi orthogonal array [OA].

Run	E'	SS' (m/min.)	SL'(N)	SD'(m)	Wear volume	S/N value of wear volume
1	Dry	30	35	600	1.5891	-4.0230
2	Dry	30	55	1200	2.3723	-7.5034
3	Dry	30	75	1800	2.9493	-9.3944
4	Dry	60	35	600	3.1055	-9.8426
5	Dry	60	55	1200	3.2998	-10.3698
6	Dry	60	75	1800	3.3011	-10.3732
7	Dry	90	35	1200	3.5381	-10.9754
8	Dry	90	55	1800	4.9983	-13.9764
9	Dry	90	75	600	4.4795	-13.0246
10	Cr LN_2	30	35	1800	0.8786	1.1242
11	Cr LN_2	30	55	600	0.8932	0.9810
12	Cr LN_2	30	75	1200	0.9257	0.6706
13	Cr LN_2	60	35	1200	1.2425	-1.8859
14	Cr LN_2	60	55	1800	1.3198	-2.4102
15	Cr LN_2	60	75	600	1.3044	-2.3082
16	Cr LN_2	90	35	1800	1.4901	-3.4643
17	Cr LN_2	90	55	600	2.1397	-6.6071
18	Cr LN_2	90	75	1200	2.2893	-7.1941

Table 5 — Response table for S/N ratio wear volume (mm^3).

Response	Level	Sliding Condition	SS'(m/min.)	SL'(N)	SD'(m)
Wv'	1	-9.943	-3.024	-4.845	-5.804
	2	-2.344	-6.198	-6.648	-6.210
	3	-	-9.207	-6.937	-6.416
	Delta	7.599	6.183	2.093	0.612
	Rank	1	2	3	4

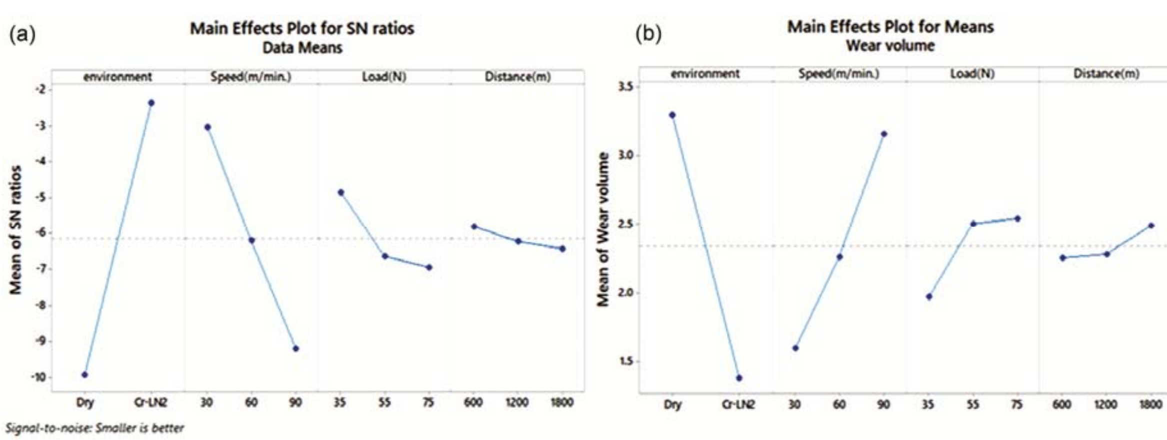

Fig. 4 — Diversification of (a) mean S/N ratio wear volume (b) means of mean wear volume with various factor levels.

distance wear volume increased. From Table 5 the highest S/N ratio was selected for an optimum value of each level. The optimized sliding parameters at E '= LN_2, SS' = 30m/min., SL' = 35N and SD' = 600m. Equations (3) and (4) were used for calculating the predicted value of each response. Where, $\overline{\delta_p}$ was the average S/N ratios of all variables δ_p was the actual calculated S/N response at optimum level, $\overline{S_{co}}$ was the average S/N ratio when variable E' (sliding condition) was at optimum level, $\overline{S_0}$ was the average S/N ratio when variable (sliding speed) was at optimum level, $\overline{L_o}$ was the average S/N ratio when variable (load) was at optimum level and $\overline{Di_o}$ was the average S/N ratio when variable (sliding distance) was at optimum level. Z_p was the predicted responses for wear volume.

$$\delta_p = \overline{\delta_p} + \left(\overline{S_{co}} - \overline{\delta_p}\right) + \left(\overline{S_o} - \overline{\delta_p}\right) + \left(\overline{L_o} - \overline{\delta_p}\right) + \left(\overline{D_{io}} - \overline{\delta_p}\right) \quad \ldots (3)$$

$$Z_p = 10^{-\delta_p/20} \quad \ldots (4)$$

Using, Eqs (3) and (4) predicted the optimum value of wear volume was 0.7574mm^3. This was enhanced by the statistical analysis of variance (ANOVA). Table of ANOVA consists of a degree of freedom (df), adjoint sum of squares (Adj SS), adjoint mean of square (Adj MS), F-Value, P-Value and percentage of contribution. ANOVA Table 7 shows that for response friction force sliding condition has the highest effect on the percentage of contribution (64.37%), next followed by sliding speed (28.42%), load (3.82%) and lastly distance (0.24%). F-value depicted the relative importance of firstly sliding condition, secondly sliding speed, thirdly sliding load and lastly sliding distance. P-value was significant for sliding condition, sliding speed and load. Since P - value was significant at the value of level equal to or less than 0.05.

3.4 Confirmation Tests

Confirmatory validity experiment was performed in accordance with the predicted parameter. This was for checking the difference between predicted optimized value and confirmation experimental value. The results are shown in Table 8

3.5 Wear of pin

Worn out pins used during dry and cryogenic sliding conditions were analysed for better understanding of wear mechanism. Figure 5(a) Field scanning electron microscope (FSEM) image depicts coating peeling, adhesives, edge fracture and small depressions during dry sliding. Figure 5(b) Field scanning electron microscope (FSEM) image shows a clean & smooth surface of the pin with a minor edge fracture during cryogenic cooling. This may be due to the low temperature generated at the interface of pin and disc. LN_2 provided a fluid film between pin and disc. This generated a lubrication effect.

Table 6 — Response table for means wear volume.

Response	Level	Sliding Condition	SS'(m/min.)	SL'(N)	SD'(m)
Wv'	1	3.293	1.601	1.974	2.252
	2	1.387	2.262	2.504	2.278
	3	-	3.156	2.542	2.490
	Delta	1.906	1.554	0.568	0.238
	Rank	1	2	3	4

Table 8 — Confirmatory test result.

Response	Optimum level of response at control factors	Predicted value of response	Actual value of response at experimental (optimized level)
Wv'	E'= LN_2, SS'= 30m/min., SL'= 35N and SD'= 600m	0.7574	0.7570

Table 7 — Analysis of variance for means of wear volume and temperature (Te').

Response	Source	DF	Adj SS	Adj MS	F-Value	P-Value	% Cont.
Wv'	E'	1	259.835	259.835	207.12	0.000	64.37
	SS' (m/min.)	2	114.709	57.354	45.72	0.000	28.42
	SL'(N)	2	15.430	7.715	6.15	0.018	3.82
	SD'(m)	2	1.162	0.581	0.46	0.642	0.29
	Error	10	12.545	1.255	-	-	-
	Total	17	403.681	-	-	-	-

3.6 Wear of Disc

Wear tracks formed on the disc were analysed during dry and cryogenic cooling. Figure 6(a) Field scanning electron microscope (FSEM) image depicts cavities, wear debris, plough and delamination during dry sliding. Figure 6(b) Field scanning electron microscope (FSEM) image shows minor cavities, plough, clean and smooth surface. This may be due to the pressurised flow of LN_2 that washed away out the debris between pin and disc. The low temperature created and maintained by LN_2 prevented the surface from contamination and deterioration.

3.7 Scanning electron microscope with energy dispersive spectroscopy SEM (EDS) and elemental mapping of major elements of wear tracks

Figure 7(a) SEM image, (b) EDS and Figure 8 show major elements of the composition of AISI D3 of wear track created during dry sliding at SS' = 90m/min, SL' = 75N & SD' = 600m. Figure 9(a) SEM image, (b) EDS and Figure10 show major elements of

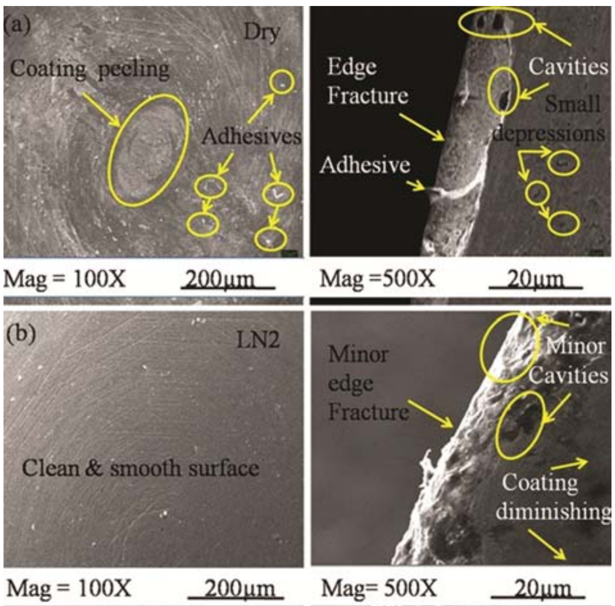

Fig. 5 — (a) Field scanning electron microscope (FSEM) image of used pin during dry sliding at sliding speed = 90m/min, sliding load = 75N, sliding distance = 600 m and (b) with LN_2 sliding distance = 1200m.

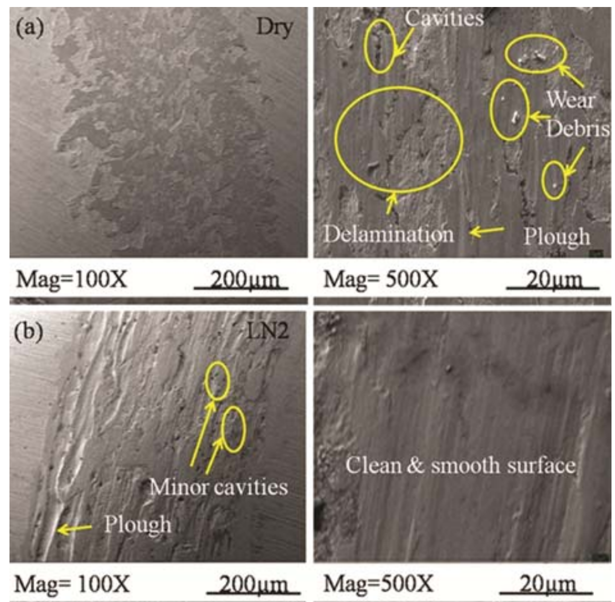

Fig. 6 — (a) Field scanning electron microscope (FSEM) image of wear tracks on disc formed during dry sliding at sliding distance = 90m/min, sliding load = 75N, sliding distance = 600m and (b) with LN_2 sliding distance = 1200m .

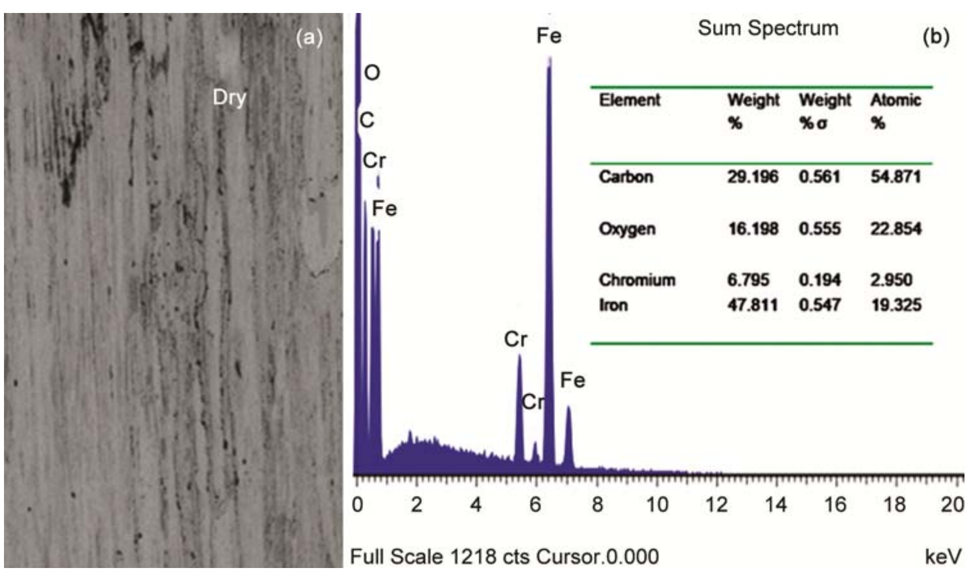

Fig. 7 — SEM image (a) and EDS graph and (b) of wear track formed during dry sliding at parameters of sliding speed = 90m/min, sliding load = 75N and sliding distance = 600m.

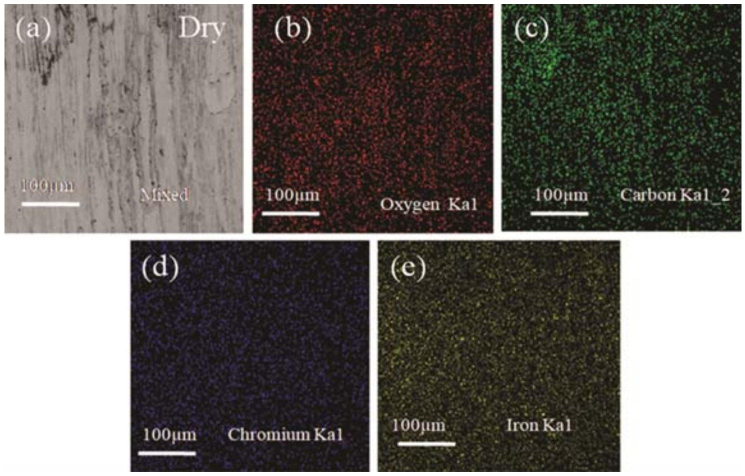

Fig. 8 — SEM image (a) elemental mapping of major elements, (b) oxygen, (c) carbon, (d) chromium and (e) iron of wear track formed during dry sliding at sliding speed = 90m/min, sliding load = 75N and sliding distance = 600m.

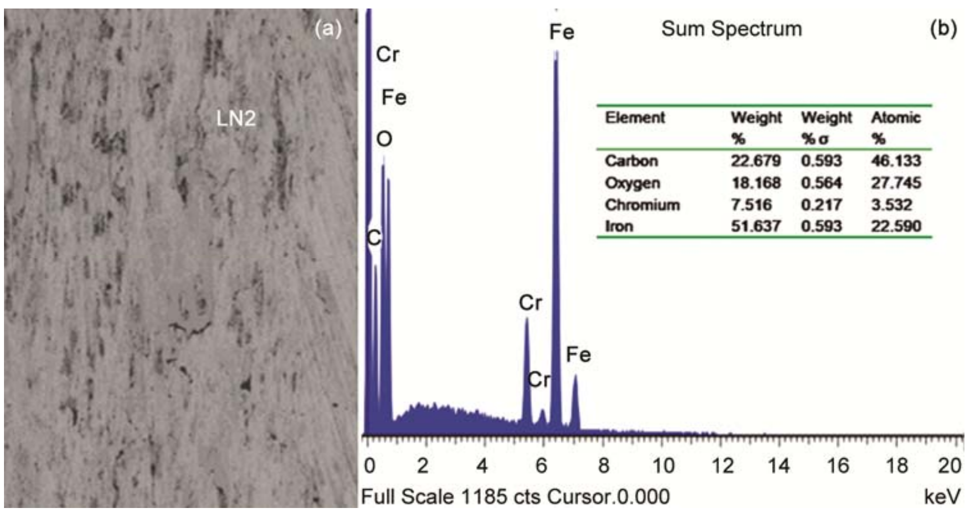

Fig. 9 — SEM image (a) and EDS graph (b) of wear track formed during cryogenic sliding with LN_2 at sliding parameters of speed = 90m/min, sliding load = 75N and sliding distance = 1200m.

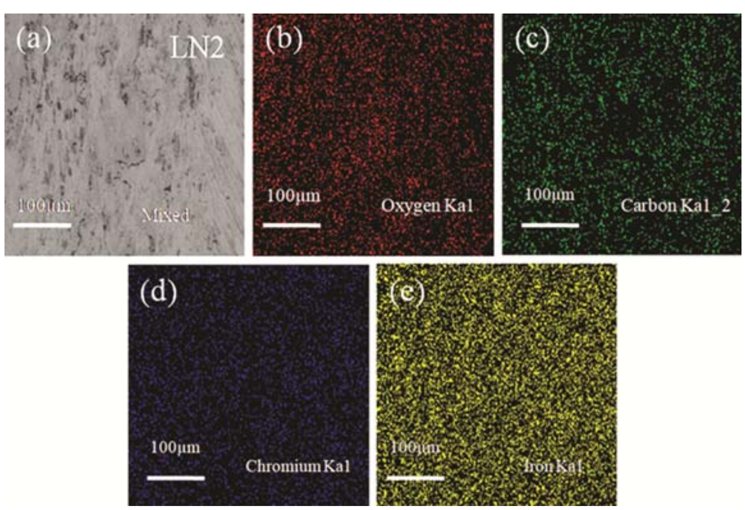

Fig. 10 — SEM image (a) elemental mapping of major elements, (b) oxygen, (c) carbon, (d) chromium and (e) iron of wear track formed during cryogenic sliding with LN_2 at sliding parameters of speed = 90m/min, sliding load = 75N and sliding distance = 1200m.

90m/min, SL' = 75N & SD' = 600m. Figure 9(a) SEM image, (b) EDS and Figure10 show major elements of the composition of AISI D3 of wear track created during cryogenic sliding with LN_2 at SS'=90m/min, SL'=75N & SD'= 1200m. It was observed that most peaks of elements have increased during cryogenic cooling and traces of nitrogen was not present. This showed that LN_2 was chemically not reactive with material[34].

4 Conclusions

In the presented research work, sliding tests are performed in accordance with Taguchi, L_{18}, DoE (Design of experiment). Pin (TiN coated tungsten carbide) and disc (AISI D3) were used on sliding pin-on-disc tribometer during dry and cryogenic cooling with LN_2. The major conclusions are summarised as follows:

(i) Wear volume loss was lower by 45-55% during cryogenic sliding with a direct supply of LN_2 at the interface of pin and disc as compared to dry sliding due to high efficiency of LN_2 in removing heat at the interface of pin and disc.

(ii) FSEM images of pin show adhesion and abrasion wear mechanism during dry sliding. Edge fracture was observed on higher magnification. But, during cryogenic sliding, the surface was clean and smooth due to the high rate of heat removing capacity of LN_2.

(iii) SEM images of wear track showed delamination, plough and cavities during dry sliding. But, during cryogenic sliding, the surface was clean and smooth due to the pressurised flow of LN_2 washed away debris from wear track.

(iv) SEM EDS of wear track showed that peaks of iron followed by oxygen. No peak of nitrogen was found. This showed that LN_2 was unreactive with disc material.

(v) Wear volume was optimized at cryogenic cooling with LN_2, sliding speed = 30m/min., sliding load = 35N and sliding distance = 600m. ANOVA revealed that cryogenic cooling was the most significant factor by 64.37%, next followed by sliding speed = 28.42%, sliding load=3.82% and sliding distance by 0.29%.

Acknowledgements

Authors are highly thankful for the help given from laboratories and workshop of Delhi Technological University and Indian Institute of Technology, Delhi, India.

References

1 Byrne G & Scholta E, *Cirp Ann-Manuf Techn*, 42(1) (1993) 471.
2 Wang Z Y & Rajurkar K P, *Wear*, 239 (2000) 168.
3 Hong S Y & Broomer, *Clean Technol Envir*, 2(3) (2014) 157.
4 Debnath S, Reddy M M & Yi Q S, *J Clean Prod*, 83 (2014) 33.
5 Hong S Y & Zaho, *Cln Prod Prcs*, 1(1999) 107.
6 Boubekri N & Foster P R, *J Manuf Technol Mana*, 212 (5) (2015) 556.
7 Pereira O, Rodriguez A, Fernandez A A I, Barreiro J & Lopezde L L N, *J Clean Prod*, 139 (2016) 440.
8 Shokrani A, Dhokia V & Newman S T, *Int J Mach Tools Manuf*, 57 (2012) 83.
9 Gupta M K & Sood P K, *J I E I Series C*, 97I (1) (2016) 63.
10 Kalyan K V B S & Choudhury S K, *J Mater*, 203 (2008) 95.
11 Dureja J S, Singh R & Bhatti M S, *Prod Manuf Res*, 2 (2014) 767.
12 Dr. Kumar M V, Kumar B K J & Rudresha N, *Mater Today Proc*, 5 (2018) 11395.
13 Viswanathan R, Ramesh S & Subburam V, *Measurement,* 120 (2018) 107.
14 Gupta M K & Sood P, *Proc IMechE Part C J Mech Eng Sci*, 231 (2017) 1445.
15 Chinchanikar S & Choudhary S K, *Int J Mach Tool Manu*, 89 (2015) 95.
16 Liew P J, Shaaroni A, Nor, Sidik A C & Yan J, *Int J Heat Mass Tran*, 114 (2017) 380.
17 Hubner W, Gradt T, Schneider T & Borner H, *Wear*, 216 (1998) 150.
18 Ostrovskaya Y L, Tukhno T P, Gamulya G D, Vvedenkij Y V& Kuleba V I, *Tribol Int*, 34 (2001) 265.
19 Iwasa Y, Ashaboglu A F, Rabinowicz E R, Tachibanat T & Kobashit K, *Cryogenics*, 37 (1997) 801.
20 Dunckle C G, Aggeleton M, Glassman J & Taborek P, *Tribol Int*, 44 (2011) 1819.
21 Subramonian B & Basu B, *Mater Sci Eng*, 415 (2006) 72.
22 Basavarajappa S, Chandramohan G & Davim J P, *Mater Des*, 28 (2007) 1393.
23 Hongato L, Hongmin J & Xumei W, *Cryogenics*, 58 (2013) 1.
24 Lan P, Gheisari R, Meyer J L & Polycarpou A, *Wear*, 398-399 (2018) 47.
25 Basu B, Manoj Kumar B V & Gilman P S, *J Mater Sci*, 44 (2009) 2300.
26 Gradt T, Schneider T, Hubner W & Borner H, *Int J Hydrog Energy,* 23 (1998) 397.
27 Theiler G & Gradt T, *Wear*, 269 (2010) 278.
28 Veenstra T T, Venhorst G C F, Burger J F, Holland H J , Brake H J M, Sirbi A & Rogalla H, *Cryogenics,* 47 (2007) 121.
29 Wang Q, Zheng F & Wang T, *Cryogenics*, 75, (2016) 19.

30 Tayeb N S EI , Yap T C & Breven P, *Tribol Int*, 43 (2010) 2345.
31 Burton J C, Taborek P & Rutledge J E, *Tribol Lett*, 23 (2006)131.
32 Subramoniana B, Kato K, Adachi K & Basu B, *Tribol Lett*, 20 (2005) 263.
33 Nandam S R, Ravikiran U & Rao A A, *Procedia Mater Sci*, 6 (2014) 296.
34 Dhananchnezian M & Kumar, *Cryogenics*, 5 (2011) 34.
35 Gupta M K, Singh G & Sood P K, *J I E I Series C*, 96 (4) (2015) 373.
36 Berminghalam M J, Kirsch J, Sun S, Palanisamy S & Dargusch M S, *Int J Mach Tools Manuf*, 51(6) (2011) 500.
37 Sivaiah P & Charkardhar D, *Cirp J Manuf Sci Techn*, 21 (2018) 86.
38 Jerold B D & Kumar M P, *Cryogenics*, 52 (2012) 569.
39 Mia M, Prithbey, Dey R, Hossain M S, Arafat Md, Asaduzzaman Md, Ullah Md S & Zobaer S M T, *Measurement*, 122 (2018) 380.
40 Katoch S, Seghal R & Singh V, *Indian J Eng Mater Sci,* 26 (2019) 112.
41 Magibalan S, Senthilkumar P, Senthilkumar C, Prabu M, *Indian J Eng Mater Sci,* 26 (2019) 43.